

Effects of Notch Radius on the Master Failure Curve of the SENB Specimens

M. Hadj Meliani^{1,a}, Z. Azari^{2,b}, G. Pluvina^{2,c} and Y.G.Matvienko^{3,d}

¹ LPTPM, FSSI, Hassiba BenBouali University of Chlef, Esalem City, 02000, Chlef, Algeria.

² LaBPS-ENIM, Ilea of saulcy 57045, Paul Verlaine university of Metz, France

³ Mechanical Engineering Research ,Academy of Sciences,101990 Moscow, Russia.

^a hadjmeliani@univ-metz.fr, ^b azari@univ-metz.fr, ^c pluvina@univ-metz.fr ^d matvienko7@yahoo.com

Keywords: U-notch, Material Failure Curve, Notch stress intensity factor, two parameter fracture.

Abstract. Stress singularities occur at crack tips, corners and material interfaces. Stress intensity factors and T-stress are coefficients in stress singular component and first regular stress term, respectively, of the William's eigenfunction expansion series. It follows the general thought used in fracture mechanics, e.g. two parameter approaches, T-stress. Fracture theories provide relationships among fracture toughness, stress, and flaw size and are used, for example, to establish acceptance standards for material defects in structures. In the present work, we extended the analysis of constraint effect in sharp cracks to notches. The influences of notch radius on the Material Failure Curve (MFC) are very disputed. Experimental investigation in LEFM had been discussed for three points bending (TPB) specimen under various U-notch radius. The notch aspect ratio was varied in the following range $a/w = 0.4, 0.5$ and 0.6 . In the first, the U-shaped notch is analyzed using the elastic solution for two dimensions geometries, including notch stress intensity factor K_ρ and constraint, T-stress under various loading conditions. Finite element (FE) analysis is performed by the commercial Castem2000 logiciel. In the second, we proposed the notch fracture mechanics and particularly the volumetric method approach in the aim to study stress distribution at the tip of TPB specimens. The Notch Stress Intensity Factor K_ρ and the effective T-stress are very detailed in this paper to determine the Material Failure Curve (MFC) for SENB specimens with various U-notches. The exploitation the $(K-T)$ crack approach, which was derived from a rigorous asymptotic solution, is developed for a notch two-parameter fracture $(K_\rho-T_{ef})$. With K_ρ as the driving force and the effective T -stress as constraint parameter, this approach has are successfully used to quantify the constraints of notch-tip fields for various proposed radius.

Introduction

It is well known that fracture resistance increases with defect tip radius and evolution can be considered using local fracture criterion particularly through the characteristic length. The characteristic length was firstly associated with notch radius in Creager and Paris [1] analysis of the stress distribution at notch tip. For rounded V-notches, analytical expression of notch tip stress distribution for elastic material was developed by Filippi et al.[2]. They introduces in this analytical expression the distance between the origin of the polar coordinates system and the notch tip r_0 . This distance r_0 depends on notch radius and notch angle. For the particular case of a zero notch angle, one finds :

$$r_0 = \frac{\rho}{2} \tag{1}$$

This value is the same which was introduced by Creager and Paris [1] for a U notch with parallel sides. Then the mode I notch stress intensity factor is given by :

$$K_{\rho,I} = \frac{1}{2} \sqrt{\pi \rho \sigma_{\theta\theta}} \left(\frac{\rho}{2}, 0 \right) \quad (2)$$

This leads to the following value of the characteristic length called here effective distance

$$X_{ef} = \frac{\rho}{2} \quad (3)$$

According to equation (3), the notch fracture toughness is a linear function of the square root of the notch radius and confirm by numerous experimental results [3]. Increase of fracture toughness with notch radius may be assumed due a low of constraint, the stress field at notch tip is strongly modified by increasing the notch radius. In order to check this assumption, we have analysis experimental results obtained by Akourri et al.[3] on SENB specimens having different notch radius and made in XC38 steel. Stress distribution at notch tip has been determined by Finite Element analysis. The constraint was measured by the value of the effective T stress, T_{ef} . Procedure of determination of this parameter and the build-up of a material master curve ($K_{\rho}-T_{ef}$) are described in [4].

Material and specimens

Notch fracture toughness has been determined on steel specimens. The material is a ductile steel (French name XC 38) with the following mechanical properties : yield stress $R_e = 304$ MPa, ultimate strength $R_m = 430$ MPa.

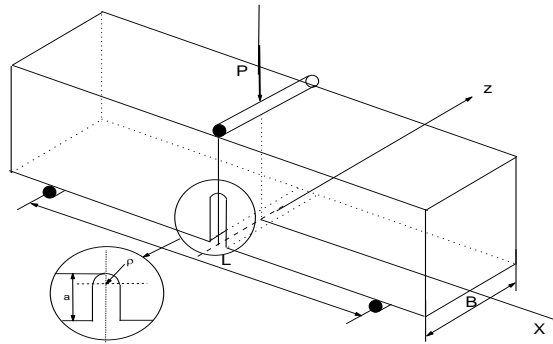


Fig.1. Geometry and loading of the three-point bend plate.

Specimens used for experiments are of SENB type. The geometry is described in Figure 1. Dimensions are listed in the following : thickness, $B = 25$ mm, width, $w = 25$ mm, length, $h = 70$ mm, ligament size, $b = 5, 10, 15, 17.5$ and 20 mm, notch opening $\alpha = 0^\circ$ and the notch radius, $0.15, 0.25, 0.5, 1, 1.5, 2$ and 4 mm. Specimens are loaded until fracture and the critical load P_c is registered. The critical load for each specimen is plotted versus the non-dimensional notch length and presented in Table 1.

Determination of notch fracture toughness

Volumetric Method, is a mesofracture criterion method derived from NFM. Experimental proofs of the validity of this method are given in reference [5]. The average stress value within the fracture

process zone is then obtained by a line method which consists to average the opening stress distribution over the effective distance. One obtains the second fracture criterion parameter called the effective stress σ_{ef} . However, it is necessary to take into account the stress gradient due to loading mode and specimen geometry. This is done by multiply the stress distribution by a weight function $\Phi(r, \chi)$ where r is the distance from notch tip and χ the relative stress gradient defined by :

$$\chi(r) = \frac{1}{\sigma_{yy}(r)} \frac{\partial \sigma_{yy}(r)}{\partial r} \quad (4)$$

Several weights functions can be used including the unit and Peterson's weight function and are described in [6]. The effective stress is finally defined as the average of the weighted stress inside the fracture process zone:

$$\sigma_{ef} = \frac{1}{X_{ef}} \int_0^{X_{ef}} \sigma_{yy}(r) \cdot \Phi(r, \chi) dr \quad (5)$$

where σ_{ef} , X_{ef} , $\sigma_{yy}(r)$ and $\Phi(r, \chi)$ are effective stress, effective distance, opening stress. In figure 2, the opening stress distribution versus distance is plotted in bi-logarithmic axes; the relative stress gradient is also plotted on the same graph. The notch stress intensity factor defined from effective distance and stress by the following relationship :

$$K_{\rho} = \sigma_{ef} \sqrt{2\pi X_{ef}} \quad (6)$$

A simple fracture criterion is obtain by using the critical notch stress intensity factor $K_{\rho,c}$ and write

$$K_{\rho} = K_{\rho,c} \quad (7)$$

The critical notch stress intensity factor is a fracture toughness values with units $MPa\sqrt{m}$, if the notch has parallel side (notch angle equal to zero) and for elastic behaviour.

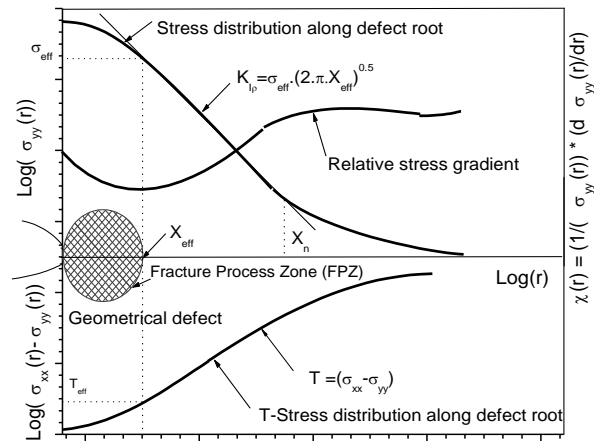


Fig.2. The notch stress intensity factor and the effective T-stress at the notch tip.

Numerical determination of effective T-stress for notches

Several methods have been proposed in literature to determine T-stress for cracked specimen. The stress difference method has been proposed by Yang et al.[7]. Chao et al [8] compute by Finite element method σ_{xx} in direction $\theta = 180^\circ$ (in the crack rear back direction) and define T stress as the value of σ_{xx} in region where value is constant. Ayatollahi et al.[9] have determined T stress by using the displacement method in finite element and obtain then a stabilised T stress distribution along ligament. Wang [10] has determined T stress by superposition of a crack free specimen with a specimen with crack faces submitted to a pressure distribution. T is then computed by the sum of two contributions, one to crack pressure distribution and the second to the difference ($\sigma_{xx}-\sigma_{yy}$) at a distance equal to crack length). In this paper, we have chosen to determine T stress in a notched body by stress difference method because it is the simplest method and widely used and then allows comparison of our results. Numerically, we use the Stress Difference Method (SDM). This method is simply based on the T stress definition:

$$T = (\sigma_{xx} - \sigma_{yy})_{r=0, \theta=0} \quad (8)$$

Examples of the computing T-stress distribution along ligament for a different specimens (CT, SENT, DCB and RT) with notches are given in Ref. [4] for a large range of non dimensional notch length a/w (0.1-0.7). Experimental procedure is based on the William's asymptotic solution Williams (1957) [11] for crack tip strains in the vicinity of a mode I crack in a planar elastic body and a strain gauge measurement technique proposed by Hadj Meliani et al. (2010) [4] for evaluating the T -stress under static loading directly from the experiments. The Notch fracture toughness transferability has been proposed as a $K_{\rho,c} - T_{eff,c}$ curve and established from the tests of four specimen types (CT, SENT, DCB and RT) made from X52 pipe steel. For more details see for example, refs [12-14].

Results and discussions

Stress distribution at notch-tip has been computed using Finite Element Method. the CASTEM™ code was used for this purpose. SENB specimen exhibits a symmetry axis. In order to reduce the number of elements and saving time computing, only half the specimen has been represented by a mesh work. Loading conditions are represented by non displacement along y axis in the ligament section. A typical, mesh type near notch-tip is presented in Figure 3.

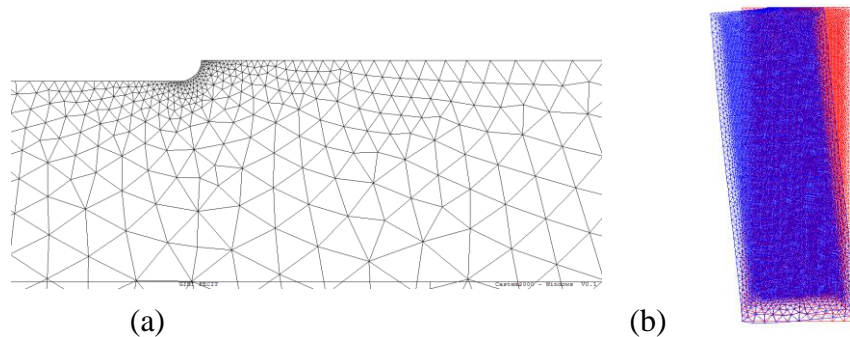


Fig.3. (a) mesh near notch-tip for SENB specimen and (b) specimen after deformation.

Figures 4 show distributions of the notch-opening stress σ_{yy} along the ligament obtained from the FEA (as denoted by symbols) for the SENB specimens with a shallow notch $a/W = 0.2$ and a deep notch of $a/W = 0.7$, respectively.

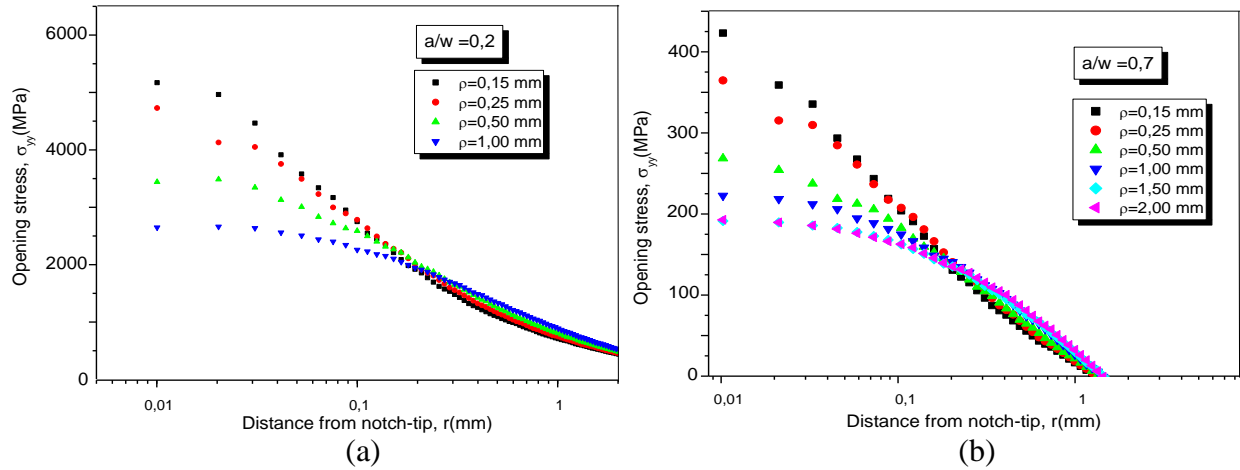


Fig.4. (a) Distribution of notch-opening stress along the uncracked ligament from the notch tip for SENB specimen with short notch $a/W = 0.2$ and (b) for long notch $a/W = 0.7$ for different notch radius.

Table 1. Recapitulation of different results for the SENB specimen.

Ratio rapport	Notch radius (mm)	Max.P _c (kN) [3]	σ_{max} (MPa)	X_{ef} (mm)	σ_{ef} (MPa)	K_{ρ} (MPa.m ^{0.5})
a/w =0,7	0,150	8,584	471,670	0,029	336,205	04,561
	0,250	9,056	400,300	0,045	282,865	04,755
	0,500	8,898	274,095	0,104	183,320	04,685
	1.000	10,359	227,760	0,141	160,215	04,768
	1,500	11,011	196,915	0,182	142,520	04,818
	2.000	12,157	195,250	0,365	137,850	06,600
a/w=0,5	0,150	24,988	2712,300	0,010	2423,200	19,203
	0,250	26,606	2179,650	0,022	1970,550	23,162
	0,500	27,752	1651,400	0,078	1270,000	28,108
	1.000	28,404	1215,600	0,162	905,000	28,866
	1,500	29,865	1050,550	0,261	755,815	30,617
	2.000	33,281	1037,500	0,570	630,000	37,693
a/w=0,2	0,150	59,932	5819,500	0,020	4968,395	55,682
	0,250	61,55	5170,000	0,040	3855,000	61,099
	0,500	63,505	3579,250	0,080	2865,850	64,236
	1.000	66,269	2752,950	0,130	2364,450	67,559
	1,500	67,415	2567,600	0,150	2240,550	68,767
	2.000	70.000	2185,350	0,270	1852,175	76,268

The opening stress distribution is presented in Fig.5 for a notch with a notch depth $a/W = 0.5$ and notch radius 2 mm. The notch stress intensity factor is calculated from equation (9). Table 1 reports the different results of notch stress intensity factor along principal direction (xx).

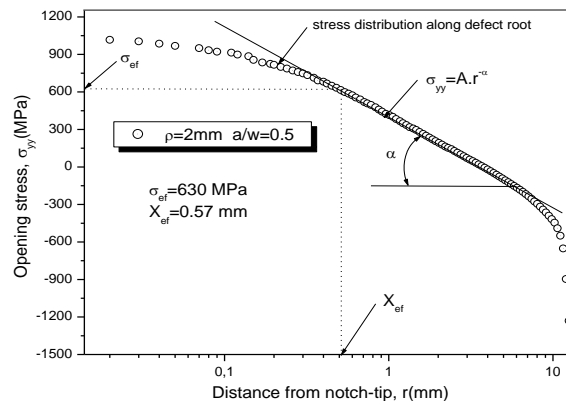


Fig.5. Stress distribution versus notch tip radius in a bilogarithmic plot ($a/W = 0.5$, $\rho=2\text{mm}$)

Influence of the notch radius on notch stress intensity factor

Numerical results of notch stress intensity factor (NSIF), for SENB specimens with different notch depth a/W , are compared to results of Akourri et al.[3] and plotted in Fig. 6. In Figure 6.a, evolution of NSIF variation allows determination critical radius ρ_c . Below this critical notch radius, critical NSIF is constant. Value $\rho_c = 1.52\text{ mm}$ is compared to $\rho_c = 0.85\text{ mm}$ from experimental results [3].

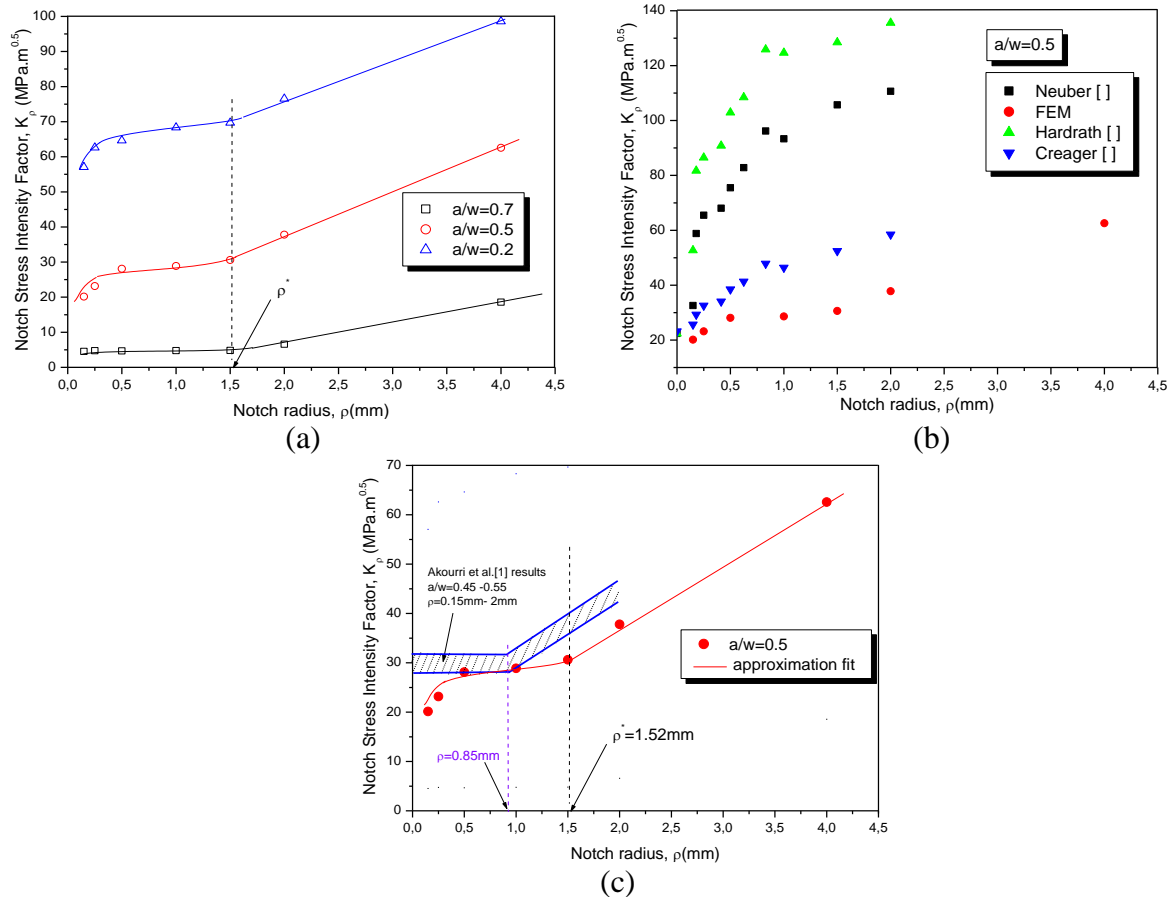


Fig. 6 (a) Evolution of the notch stress intensity factor versus the radius for the SENB specimen ($a/w = 0.2, 0.5$ and 0.7), (b) numerical results compared to different methods in the literature and (c) example of the numerical MFC for $a/w=0.5$ compared to experimental Akourri results.

The numerical results are compared Neuber, Hardrath and to Creager equation, Fig.6.b. Evolution of the notch stress intensity factor as a function of notch root radius shows an absolute minimum with the abscissa ρ ranging between 0 and 0.25 mm (Fig. 6(c)). Similarly, we notice that for radius values below ρ_c , the stress intensity factor decreases linearly with ρ and not constant as expected by equation (2). This results explains probably the fact that NSIF plateau is not found in some experimental results. Beyond this critical abscissa, notch stress intensity factor increases with ρ as expected by equation (2). For low a/W ratio, critical NSIF becomes approximately constant for a radius ranging between 0.25 and 1.52 mm.

Material Failure Curve

Numerical assessment points ($K_{\rho,c}, T_{ef,c}$) for SENB specimen geometry with notch aspect ratio ($a/w = 0.2, 0.5$ and 0.7) are summarized in Figure 9. These points allow constructing a material failure curve called also a material master curve for different notch radius. The increasing of the notch stress intensity factor with the presence of constraint is in the range 27%– 49 % with the increasing of the notch tip for $\rho = 0.15$ to $\rho = 2$ mm. One notes that the material failure curve for the X38 steel is very sensitive to notch tip.

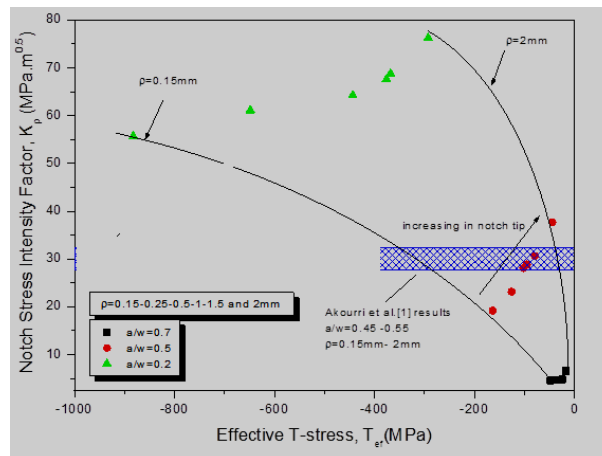


Fig.7. Material failure curve for the SENB specimen with $a/W=0.2, 0.5$ and 0.7 .

Notch Stress Intensity Factor (NSIF) with constraint

A linear increasing of the critical notch stress intensity factor K_p with constraint parameter is noted in Figure 7 for SENB specimen with non dimensional crack length $a/W= 0.2 ; 0.5$ and 0.7 . These figure show also a decreasing of notch fracture toughness with ligament size for different notch radius. The transferability problem has been expressed as a curve $K_{\rho,c} = f(T_{ef}, \rho)$ where T_{ef} is the constraint parameter and ρ the notch radius. A polar coordinate system (r, θ) with origin at the notch tip is used. Notch stress intensity factor evolution with constraint is presented in the Figure 8.b for different notch depth. Increasing of the NSIFs is about 15.8% for short notch to 7% for very deep notch. Thus, the master curve is a way to take into account effect of constraint on notch fracture toughness and solve the transferability problem which occurs when fracture resistance is determined with other constraint conditions than structure or component.

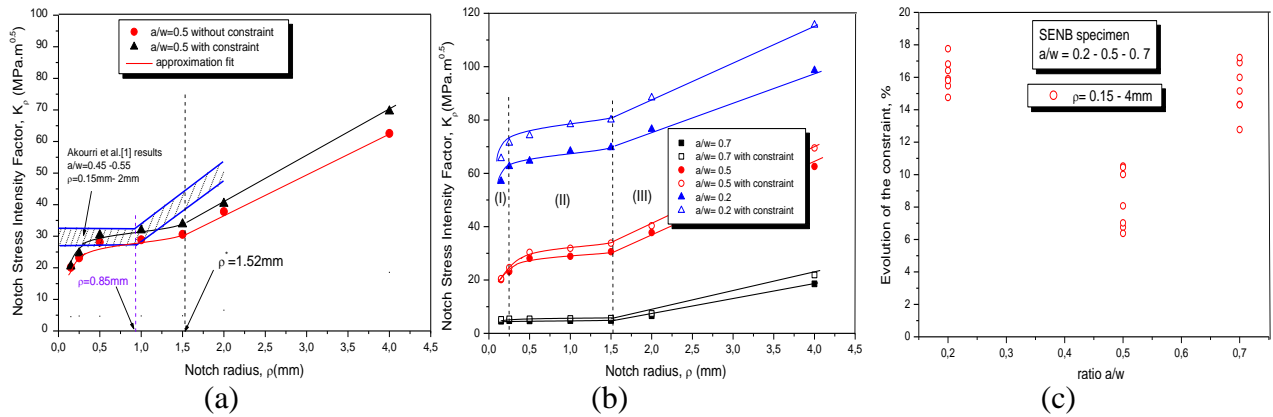


Fig. 8. (a) Evolution of critical notch stress intensity factor ($K_{\rho,c}$) with the presence of constraint (T -stress) for SENB specimen ($a/W = 0.5$), (b) with different notch radius ($a/W = 0.2, 0.5$ and 0.7) and the error of the notch stress intensity with the notch radius.

Conclusion and remarks

Dependence of notch fracture toughness with notch radius has been obtained using the Material Failure Curve's relationship. Effect of notch root radius through constraint on fracture resistance consists of three phases: in the first one, increasing of the NSIF for very short notch ($\rho < 0.2$ mm), in second phase, it remains constant until a critical value of the notch radius; in the third phase $K_{\rho,c}$ increases linearly with ρ . The difference between results given in Akourri et al. [3] reference and the above mentioned numerical results are explained by the effect of constraint (not taken into account in [3]). The material failure curve is a tool introduced in Notch Failure Assessment Diagram (NFAD) as an extension of the FAD generally used for crack-like defect. It is less conservative because it takes into account the real defect acuity.

References

- [1] Creager, M. and Paris, P. C. International Journal of Fracture. Vol. 3, pp. 247-252, (1967).
- [2] Filippi, S., Lazzarin, P., Tovo, R. Int J Solid Struct. 39:4543-4565 (2002).
- [3] Akourri, O., Elayachi, I., Pluvinage, G. IREME, Vol. 1, N°6 November (2007).
- [4] Hadj Meliani M., Pluvinage G., Matvienko Y.G. Eng. Frac. Mechanics. 77:1682-1692 (2010).
- [5] Pluvinage G. Nuclear Engineering and Design. 185:173-84 (1998).
- [6] Adib H., Jallouf S., Schmitt C., Carmasol A., Pluvinage G. Int J. P. V. Piping. 84: 123-31 (2007).
- [7] Yang, B., Ravi-Chandar, K. Engng Fract Mech. 64:589-605 (1999).
- [8] Chao, Y.J., Liu, S., and Broviak, B.J. ASME-PVP 393, 113-120 (1999).
- [9] Ayatollahi, M.R., Pavier, M.J., and Smith, D.J. Int. J. of Fracture. 91, 283-298 (1998).
- [10] Wang X. Eng Fract Mech. 70: 731-756 (2003).
- [11] Williams ML. ASME J Appl Mech; 24 : 109-14 (1957).
- [12] Hadj Meliani M., Matvienko Yu.G., Pluvinage G. Engng Failure Analysis; 18: 271-283 (2011).
- [13] Hadj Meliani M., Azari Z., Pluvinage G. Engng Failure Analysis; 17: 1117-1126 (2010).
- [14] Hadj Meliani M., Pluvinage G., Matvienko Y.G. Int. J. of Fracture. 167:173-182 (2011).